Carbohydrate Research, 232 (1992) 327–339
Elsevier Science Publishers B.V., Amsterdam

Note

Conformational analysis of the trisaccharide components of the repeating units of the capsular polysaccharides of *Streptococcus pneumoniae* types 19F and 19A *

Pierangela Ciuffreda [a], Diego Colombo [a], Fiamma Ronchetti [a] and Lucio Toma [b]

[a] *Dipartimento di Chimica e Biochimica Medica, Università di Milano, Via Saldini 50, 20133 Milano (Italy)*
[b] *Dipartimento di Chimica Organica, Università di Pavia, Viale Taramelli 10, 27100 Pavia (Italy)*

(Received November 1st, 1991; accepted February 10th, 1992)

The repeating units of the capsular polysaccharides of *Streptococcus pneumoniae* type 19F and 19A, which are responsible for the immunogenic activity, have the following structures [1].

→ 4)-β-D-Man*p*NAc-(1 → 4)-α-D-Glc*p*-(1 → 2)-α-L-Rha*p*-(1-PO_4^- → (19F)

→ 4)-β-D-Man*p*NAc-(1 → 4)-α-D-Glc*p*-(1 → 3)-α-L-Rha*p*-(1-PO_4^- → (19A)

Following the synthesis [2] of the trisaccharide components, modeling studies have been undertaken in order to obtain information on the geometrical requirements necessary for their biological function. As a first step, we now report the conformational analysis of the model trisaccharide glycosides methyl *O*-(2-acetamido-2-deoxy-β-D-mannopyranosyl)-(1 → 4)-*O*-α-D-glucopyranosyl-(1 → 2)-α-L-rhamnopyranoside (**1**) and methyl *O*-(2-acetamido-2-deoxy-β-D-mannopyranosyl)-(1 → 4)-*O*-α-D-glucopyranosyl-(1 → 3)-α-L-rhamnopyranoside (**2**), which were synthesised by the procedures described [2]. The structures were confirmed by 500-MHz ^{1}H-NMR spectroscopy and the spectral data are reported in Table I.

The conformational analysis of carbohydrates has been performed by several theoretical methods [3], including restrained (HSEA program [4]) and unrestrained procedures (MM2 program [5]). The former program is more rapid, but the latter gives more reliable results: an appropriate combination should allow reliable results to be obtained in reasonably short times.

Correspondence to: Professor L. Toma, Dipartimento di Chimica Organica, Università di Pavia, Viale Taramelli 10, 27100 Pavia, Italy.

* Presented at EUROCARB VI, 6th European Symposium on Carbohydrate Chemistry, Edinburgh, 8–13 September, 1991.

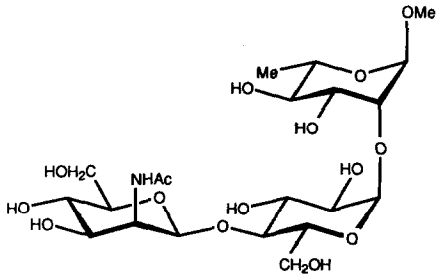

1

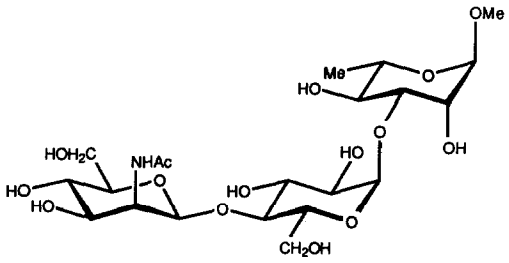

2

The modeling of **1** and **2** started with each glycosidic linkage and HSEA calculations. Energy maps, as a function of the dihedral angles ϕ and ψ for each of the three disaccharide subunits β-D-Man*p*NAc-(1 → 4)-α-D-Glc*p* (**3**), α-D-Glc*p*-(1 → 2)-α-L-Rha*p* (**4**), and α-D-Glc*p*-(1 → 3)-α-L-Rha*p* (**5**), were calculated first. The co-ordinates were taken from the crystallographic data for 2-acetamido-2-deoxy-D-mannose [6], methyl α-D-glucopyranoside [7], and α-L-rhamnopyranose [8]. The orientation of the NAc group of ManNAc was set with the C-2–H-2 and the C=O bonds eclipsed, as found in the X-ray structure, and the NH proton was included in the calculations. Following a standard approximation, HO-6 of the Glc and ManNAc residues were removed in order to provide symmetrical ring substituents. The ϕ/ψ maps are reported in Fig. 1 as isocontour levels at 1, 4, 7, and 10 kcal/mol above the global minimum, whereas the data of the minimum energy conformation are reported in Table II.

The most populated ϕ/ψ regions of **4** and **5** have a similar shape, and the two compounds have similar values of ϕ and ψ for their global and unique minima (conformers **4A** and **5A**, respectively). Conversely, the map of **3**, as expected for a β-linked disaccharide, is different in that, besides the global minimum at ϕ/ψ 62°/ − 7° (conformer **3A**), two somewhat high-energy minima were located at ϕ/ψ 65°/ − 148° and 34°/169° (conformers **3B** and **3C**, respectively), indicating for **3** a certain degree of freedom of rotation at the glycosidic linkage, particularly along the ψ angle.

HSEA-calculated ϕ/ψ energy surfaces contain deep wells due to the fact that bonds and angles inside each residue are not allowed to relax. In principle, such relaxation, allowed by fully unrestrained methods, could result in the accessibility of regions of the energy maps apparently forbidden by HSEA. However, complete exploration of the conformational space of saccharides with a fully unrestrained method through determination of the ϕ/ψ maps with a 5° grid, as usually made by HSEA, is so time consuming that alternative procedures have to be followed. Therefore, the program MM2(85), updated with the last list of parameters, was used as a fully unrestrained method for the analysis of 3 *.

* The MM2 program was tested first on the monosaccharide structures and the following geometrical data were obtained (X-ray data[6,7] in parentheses); β-D-ManNAc-OMe: C-1–O-1 1.393 Å (1.388), C-1–O-5 1.420 (1.427), C-1–O-1–Me 113.2° (−), H–N–C-2–H-2 175° (163); α-D-Glc-OMe: C-1–O-1 1.407 Å (1.401), C-1–O-5 1.409 (1.414), C-1–O-1–Me 113.3° (113.9).

TABLE I

^{1}H-NMR data (δ in ppm, J in Hz) for solutions of **1** and **2** in D_2O

Compound	H-1″	H-2″	H-3″	H-4″	H-5″	H-6″a	H-6″b	NAc	H-1′	H-2′	H-3′
1	4.81	4.48	3.73	3.45	3.38	3.75	3.86	2.00	4.92	3.50	3.82
2	4.81	4.47	3.75	3.45	3.38	3.75	3.86	2.00	4.97	3.54	3.83
	H-4′	H-5′	H-6′a	H-6′b	H-1	H-2	H-3	H-4	H-5	H-6,6,6	OMe
1	3.61	3.99	3.66	3.61	4.73	3.87	3.75	3.42	3.63	1.24	3.33
2	3.62	3.94	3.68	3.62	4.67	4.05	3.69	3.46	3.63	1.24	3.33
	$J_{1'',2''}$	$J_{2'',3''}$	$J_{3'',4''}$	$J_{4'',5''}$	$J_{5'',6''a}$	$J_{5'',6''b}$	$J_{6''a,6''b}$	$J_{1',2'}$	$J_{2',3'}$	$J_{3',4'}$	
1	1.4	4.3	9.3	10.0	2.1	5.6	11.4	3.6	9.3	9.3	
2	1.4	4.3	9.3	10.0	2.1	5.7	11.4	3.6	9.3	9.3	
	$J_{4',5'}$	$J_{5',6'a}$	$J_{5',6'b}$	$J_{6'a,6'b}$	$J_{1,2}$	$J_{2,3}$	$J_{3,4}$	$J_{4,5}$	$J_{5,6}$		
1	10.0	2.1	3.6	12.2	2.1	3.8	9.3	9.3	6.5		
2	10.0	2.1	3.6	12.2	2.1	3.8	9.3	9.3	6.5		

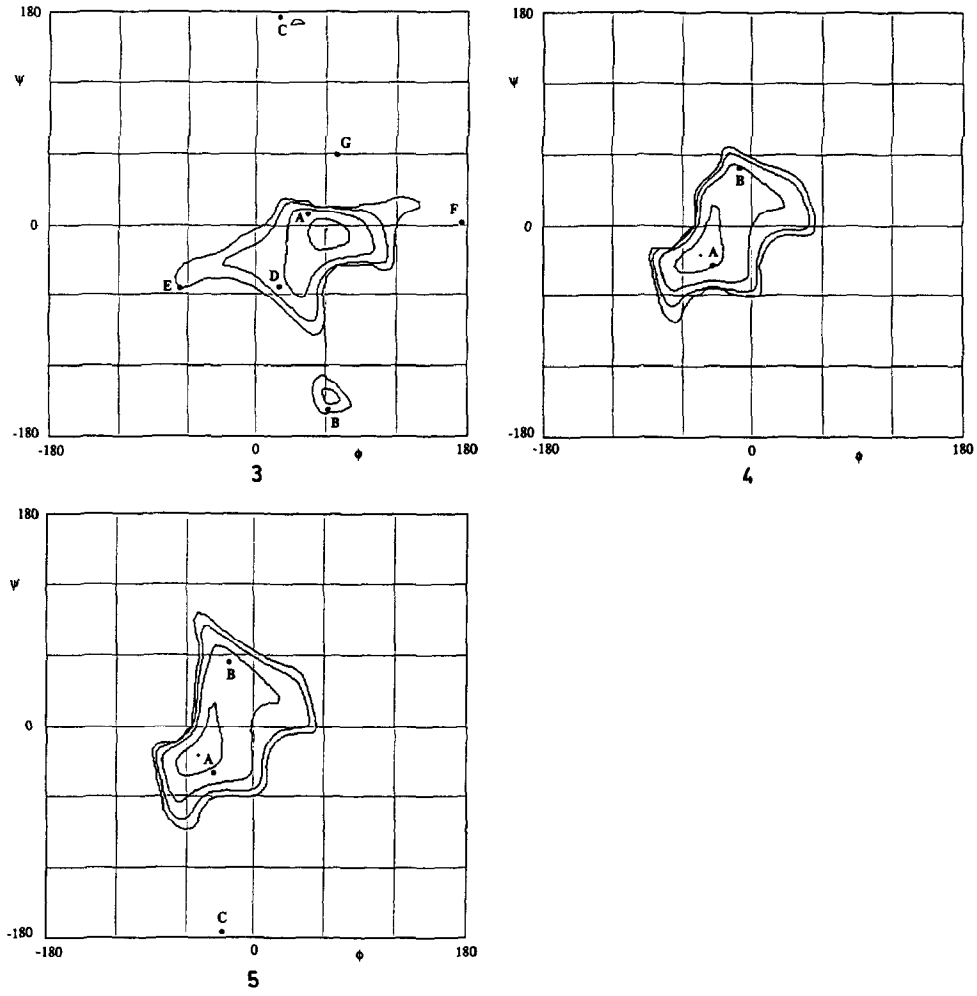

Fig. 1. Isoenergy contour diagram for the rotation of ϕ and ψ for **3–5** as calculated by the HSEA program: (●) indicates the minimum-energy conformations as calculated by the MM2 program.

The following procedure was applied. The global minimum found with HSEA was chosen as the starting geometry for the MM2 program, and all the exchangeable hydrogen atoms and the oxygen lone pairs not taken into consideration by the former method were added to the structure. After a first optimisation, all the degrees of freedom different from ϕ/ψ, i.e., the hydroxymethyl and the hydroxyl orientations, were varied randomly in order to produce new starting geometries that were submitted to complete minimisation, yielding **3A** as the lowest energy conformation. From this structure, by rigid rotation around the glycosidic bonds, 36 starting geometries were generated, which cover the entire ϕ/ψ map with a 60° grid. When these geometries were allowed to relax fully, seven local minima within

TABLE II

Data on the minimum-energy conformations of **3–5** as calculated by the HSEA program

Compound	Conformation	ϕ/ψ (°)	E_{rel} (kcal/mol)	H–H distances	< 3 Å
3	**3A**	62/−7	0.0	H-1′–H-4	2.37
				H-1′–H-6	2.36
	3B	65/−148	6.2	H-1′–H-3	2.08
				H-5′–H-3	2.45
	3C	34/169	9.8	H-1′–H-3	1.87
				H-1′–H-5	2.05
				H-5′–H-5	2.57
				H-6′–H-6	2.87
4	**4A**	−45/−26	0.0	H-1′–H-1	2.33
				H-1′–H-2	2.49
5	**5A**	−49/−26	0.0	H-1′–H-2	2.33
				H-1′–H-3	2.55

a range of 5 kcal/mol above the global minimum, including **3A**, were obtained. The convergence criterion of MM2 usually fails to locate the true minima for such molecules as di- or tri-saccharides because the program sometimes stops at values of ϕ and ψ several degrees from the true minima. In order to overcome this

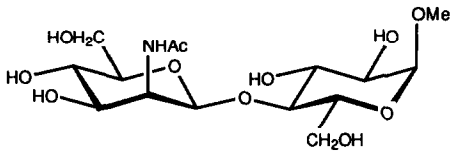

3

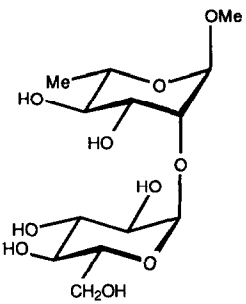

4

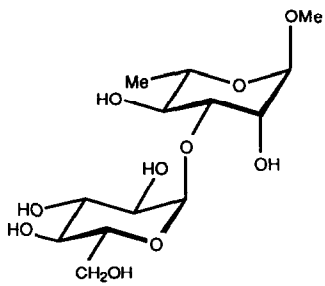

5

problem, local searches around the point in which the program had stopped were performed with the single- or double-driver option of MM2, using incremental steps of 1° for ϕ and/or ψ until a point was located which was surrounded only by points with higher values of energy. Furthermore, for each of the minima, all of the exocyclic torsional angles and the hydroxyl orientations were optimised.

The same procedure was then applied to **4** and **5**. In Fig. 1, the points indicate the positions of the conformations found as minima, and Table III contains the relative energy and proportion of each conformation. Whereas three minima for **3** were located by HSEA with relative energies of 0.0, 6.2, and 9.8 kcal/mol, seven local minima were located by MM2 within a range of 5 kcal/mol, three of which (**3A–3C**) correspond to those found by HSEA although the energy differences are smaller. Conformer **3D**, the second minimum, is near to the global minimum and is inside the HSEA 10 kcal/mol-isoenergy level, whereas conformers **3E–3G**, not recognised by HSEA as minima, are high-energy, largely unpopulated local minima. For **4** and **5**, MM2 gave the global minimum near to that found by HSEA, and a second minimum inside the HSEA 10 kcal/mol-isoenergy curve. The third minimum of **5**, outside of this curve, was almost unpopulated.

Comparison of the results obtained by MM2 and HSEA indicates that the latter method fails to locate some minima. However, the HSEA-allowed region (i.e., the region inside the 10 kcal/mol-isocontour curve) contains all the significantly populated conformations found by the former method. When, as for **3**, HSEA predicts more than one allowed region and more than one local minimum, these minima are also recognised as such by MM2. Thus, a good strategy involves the determination of the allowed regions of the ϕ/ψ maps for each glycosidic linkage by HSEA and a reinvestigation only of these regions by MM2.

The study of the conformations of **1** and **2** was undertaken with MM2 by optimisation of the starting geometries obtained by all combinations of the ϕ/ψ values found as minima for the two glycosidic linkages. After a first optimisation, all the possible orientations of the hydroxymethyl and hydroxyl groups were optimised further in each minimum. Tables IV and V contain the data on the local minima found in the range up to 3 kcal/mol above the global minima. The global minima of **1** and **2**, which account for $> 50\%$ of each population, have the geometry at the two glycosidic linkages that corresponds to those found for the global minima of the corresponding component disaccharides **3–5**, indicating a limited reciprocal influence of the two outer residues when the two molecules assume the minimum-energy conformations **1AA** and **2AA**, respectively. Inter-residue hydrogen–hydrogen distances of < 3 Å are also given in Tables IV and V, and the observed intra- and inter-residue NOEs are reported in Table VI *.

* The energy and the geometry in the points of the conformational space of **1** and **2** close to the local minima reported in Tables IV and V were determined as a function of ϕ_1 and ψ_1. These angles were "driven" (increments of 10°) near each minimum until points with $E_{rel} \geq 3$ kcal/mol were reached. From the ensembles of all the conformers of the 10° grid having $E_{rel} \leq 3$ kcal/mol, using the r^{-6} dependence, the following expected NOE values for irradiation of H-1″ were calculated (reference: H-5″): **1** H-3′, 1.1%; H-4′, 6.2%; H-5′, 0.5%; **2** H-3′, 0.8%; H-4′, 6.0%; H-5′, 0.3%.

TABLE III

Data on the minimum energy conformations of **3**–**5** as calculated by the MM2 program

Compound	Conformation	ϕ/ψ (°)	C-1′–O-*X* (Å)	C-1′–O-5′ (Å)	C-1′–O-*X*–C-*X* (°)	O-5′–C-5′–C-6′–O-6′ (°)	H–N–C-2′–H-2′ (°)	E_{rel} (kcal/mol)	Percentage
3	**3A**	44/9	1.392	1.419	114.5	−63	−174	0.0	76.3
	3B	62/−158	1.395	1.411	118.6	60	−173	2.5	1.1
	3C	19/176	1.394	1.419	116.5	60	−174	1.8	3.8
	3D	19/−53	1.391	1.420	116.4	61	−176	0.8	18.5
	3E	−67/−55	1.406	1.407	117.5	61	176	3.4	0.2
	3F	175/1	1.399	1.410	117.9	−63	164	4.3	< 0.1
	3G	70/59	1.392	1.410	119.5	60	−170	4.5	< 0.1
4	**4A**	−34/−35	1.405	1.410	114.4	61		0.0	90.4
	4B	−12/49	1.407	1.409	116.0	−56		1.3	9.6
5	**5A**	−36/−40	1.406	1.410	114.3	−63		0.0	96.5
	5B	−23/54	1.404	1.410	116.6	61		2.0	3.4
	5C	−28/−175	1.404	1.410	117.9	61		4.3	< 0.1

TABLE IV

Data on the minimum-energy conformations of **1** as calculated by the MM2 program

Conformation	ϕ_1/ψ_1 [a] (°)	ϕ_2/ψ_2 [b] (°)	C-1″–O-4′ (Å)	C-1″–O-5″ (Å)	C-1″–O-4′–C-4′ (°)	O-5″–C-5″–C-6″–O-6″ (°)	H–N–C-2′–H-2′ (°)	C-1′–O-2 (Å)	C-1′–O-5′ (Å)	C-1′–O-2–C-2 (°)	O-5′–C-5′ C-6′–O-6′ (°)	E_{rel} (kcal/mol)	Percentage	Inter-residue short H–H distances (Å)
1AA	44/9	−35/−35	1.392	1.419	114.5	−63	−172	1.406	1.409	114.3	−62	0.0	52.9	H-1″–H-4′ 2.28 H-1″–H-6′ 2.54 H-1′–H-1 2.22 H-1′–H-2 2.41
1CA	23/177	−41/−34	1.394	1.419	116.6	61	−173	1.405	1.409	114.7	64	0.6	19.5	H-1″–H-3′ 2.05 H-1″–H-5′ 2.40 H-1′–H-1 2.23 H-1′–H-2 2.48
1DA	19/−53	−35/−35	1.391	1.420	116.4	61	−173	1.405	1.408	114.3	−66	0.8	13.5	H-1″–H-4′ 2.28 H-1′–H-1 2.22 H-1′–H-2 2.41
1CB	23/176	−15/48	1.394	1.419	116.7	59	−173	1.406	1.408	116.3	64	1.4	5.2	H-1″–H-3′ 2.06 H-1″–H-5′ 2.36 H-1′–H-2 2.22
1AB	43/9	−13/49	1.392	1.419	114.4	−63	−172	1.407	1.408	116.0	59	1.5	3.9	H-1″–H-4′ 2.27 H-1″–H-6′a 2.71 H-1″–H-6′b 2.50 H-1′–H-2 2.23
1BA	56/−160	−29/−33	1.394	1.413	119.1	64	−171	1.406	1.411	114.1	−66	1.7	2.9	H-1″–H-3′ 2.24 H-1′–H-1 2.30 H-1′–H-2 2.31
1DB	19/−54	−13/49	1.391	1.420	116.3	61	−175	1.406	1.406	115.8	60	2.2	1.2	H-1″–H-4′ 2.29 H-1′–H-2 2.22
1BB	62/−159	−12/50	1.394	1.411	119.0	62	−172	1.408	1.408	115.6	60	2.5	0.8	H-1″–H-3′ 2.30 H-1′–H-2 2.23

[a] ϕ_1 H-1″–C-1″–O-4′–C-4′, ψ_1 C-1″–O-4′–C-4′–H-4′. [b] ϕ_2 H-1′–C-1′–O-2–C-2, ψ_2 C-1′–O-2–C-2–H-2.

TABLE V

Data on the minimum-energy conformations of **2** as calculated by the MM2 program

Conformation	ϕ_1/ψ_1 [a] (°)	ϕ_2/ψ_2 [b] (°)	C-1″–O-4′ (Å)	C-1″–O-5″ (Å)	C-1″–O-4′–C-4′ (°)	O-5″–C-5″–C-6″–O-6″ (°)	H–N–C-2′–H-2′ (°)	C-1′–O-3 (Å)	C-1′–O-5′ (Å)	C-1′–O-3–C-3 (°)	O-5′–C-5′ C-6′–O-6′ (°)	E_{rel} (kcal/mol)	Percentage	Inter-residue short H–H distances (Å)
2AA	44/9	−37/−40	1.392	1.419	114.7	−63	−172	1.406	1.409	114.4	−63	0.0	59.3	H-1″–H-4′ 2.29 H-1″–H-6′ 2.51 H-1′–H-2 2.21 H-1′–H-3 2.50
2CA	21/176	−45/−42	1.394	1.419	116.4	61	−173	1.405	1.408	115.0	64	0.6	20.5	H-1″–H-3′ 2.06 H-1″–H-5′ 2.34 H-1′–H-2 2.20 H-1′–H-3 2.64
2DA	20/−53	−38/−40	1.390	1.420	116.5	61	−175	1.405	1.407	114.3	−65	0.9	14.1	H-1″–H-4′ 2.29 H-1′–H-2 2.20 H-1′–H-3 2.51
2BA	64/−157	−34/−36	1.396	1.411	118.8	−60	−172	1.406	1.410	114.0	−66	1.7	3.3	H-1″–H-3′ 2.30 H-1′–H-2 2.26 H-1′–H-3 2.40
2AB	44/9	−22/54	1.392	1.419	114.6	−63	−172	1.404	1.410	116.7	−63	2.0	1.9	H-1″–H-4′ 2.28 H-1″–H-6′ 2.52 H-1′–H-3 2.29
2DB	20/−54	−21/53	1.391	1.420	116.4	61	−175	1.404	1.408	116.6	−66	2.8	0.5	H-1″–H-4′ 2.29 H-1′–H-3 2.28
2CB	21/176	−29/59	1.394	1.419	116.4	60	−173	1.401	1.410	117.4	64	3.0	0.4	H-1″–H-3′ 2.07 H-1″–H-5′ 2.34 H-1′–H-3 2.35

[a] ϕ_1 H-1″–C-1″–O-4′–C-4′, ψ_1 C-1″–O-4′–C-4′–H-4′. [b] ϕ_2 H-1′–C-1′–O-3–C-3, ψ_2 C-1′–O-3–C-3–H-3.

TABLE VI

NOE data for **1** and **2**

Compound	Irradiated proton	Observed proton	%	Compound	Irradiated proton	Observed proton	%
1	H-1″	H-2″	5.1	**2**	H-1″	H-2″	3.9
		H-3″	3.2			H-3″	1.6
		H-5″	5.3			H-5″	5.0
		H-3′	1.2			H-3′	1.0
		H-4′	5.2			H-4′	4.1
		H-6′	1.1			H-6′	1.0
	H-1′	H-2′	6.0		H-1′	H-2′	4.7
		H-1	4.1			H-2	5.6
		H-2	4.4			H-3	2.7
	H-1	H-1′	3.9		H-1	H-2	4.3
		H-2	2.5			MeO	1.0
		MeO	1.4				

Significant NOEs between H-1″ and H-4′ were observed for **1** and **2** accompanied by smaller NOEs between H-1″ and H-3′,6′. Whereas the short distance H-1″–H-6′ is observed in the calculated conformations **1AA** and **2AA**, the NOE of ~ 1% between H-1″ and H-3′ reflects an ~ 20% contribution (from the calculated MM2 energies) of the conformers **1CA** and **2CA** that have the same geometry as **1AA** and **2AA** at the Glc-Rha linkage, but a different geometry at the ManNAc-Glc linkage. Thus, an exchange between different conformations must be taken into account in the interpretation of the observed NOE data. No small NOE was observed on irradiation of the Glc H-1, which indicates the Glc-Rha linkage to be rigid. Fig. 2 shows the three-dimensional plots of the conformations **1AA**, **1CA**, **2AA**, and **2CA**.

The above cAnformational study of **1** and **2** indicates a rather rigid conformation at the Glc-Rha linkages (ϕ and ψ in the range $-35°$ and $-40°$), whereas the ManNAc-Glc linkage is more flexible, which will have implications for the modeling of larger portions of the polysaccharides.

EXPERIMENTAL

The ^{1}H-NMR spectra (500.13 MHz) were recorded with a Bruker AM 500 spectrometer on 0.05 M solutions of **1** and **2** in D_2O at 40°, with the data size of 32k, and were referenced to HDO at 4.55 ppm. NOE experiments were performed in the difference mode with 16k data points, a pre-saturation time of 1.5 s, a relaxation delay of 3.1 s, a sweep width of 5582 Hz, and 7232 scans. Optical rotations were measured with a Perkin–Elmer 241 polarimeter. The HSEA program [4] was used to estimate minimum-energy conformations and rotational freedom at the glycosidic linkage of the disaccharides **3–5**. The torsional angles ϕ and

ψ were defined by H-1′–C-1′–O-X–C-X and C-1′–O-X–C-X–H-X, respectively ($X = 4$ for **3**, $X = 2$ for **4**, $X = 3$ for **5**). The bond angle C-1′–O-X–C-X was set to 117°. The MM2(85) program [5] was used for a more detailed conformational analysis of **1–5**. The glycosidic dihedral angles of **1–2** are defined as reported in Tables IV and V. Geometries were optimised without any constraint at a dielectric constant $\epsilon = 78$.

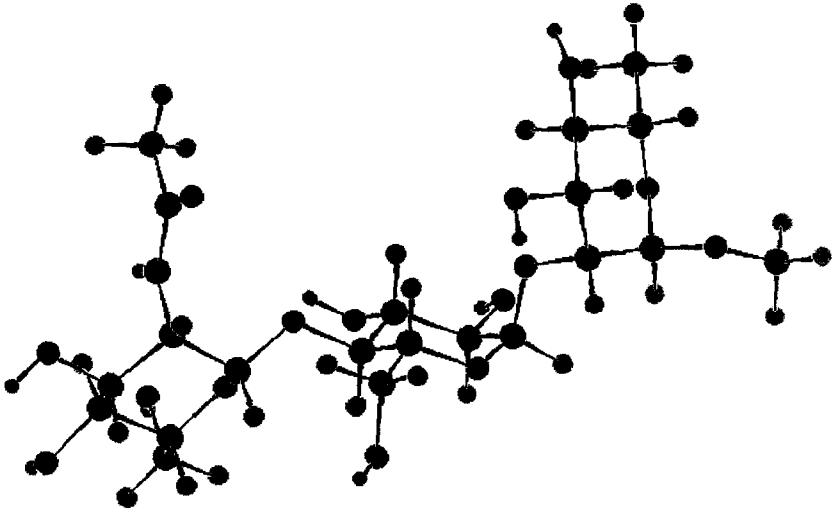

1AA

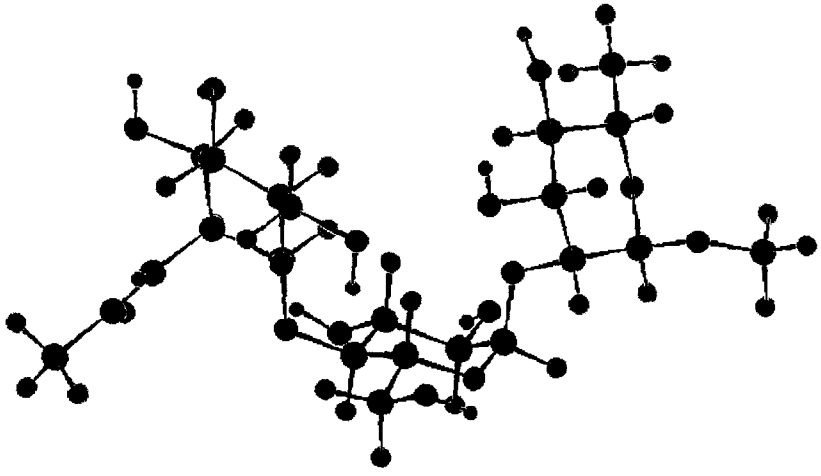

1CA

Fig. 2. Three-dimensional plots of the most populated conformations of **1** and **2**.

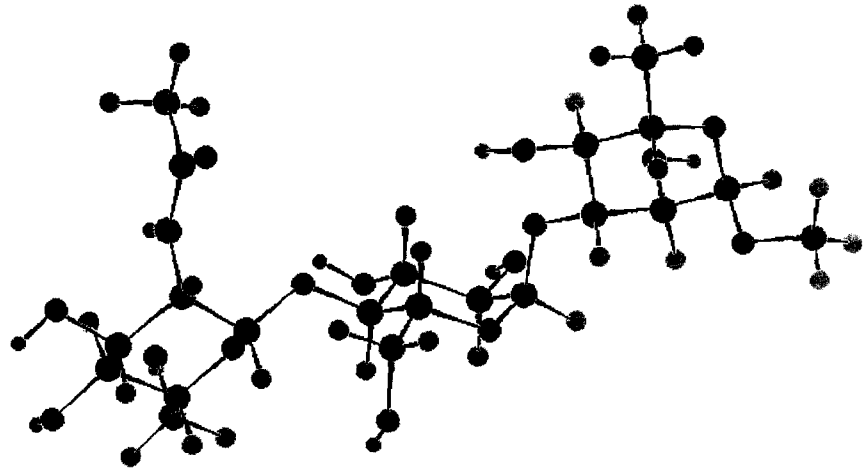

2AA

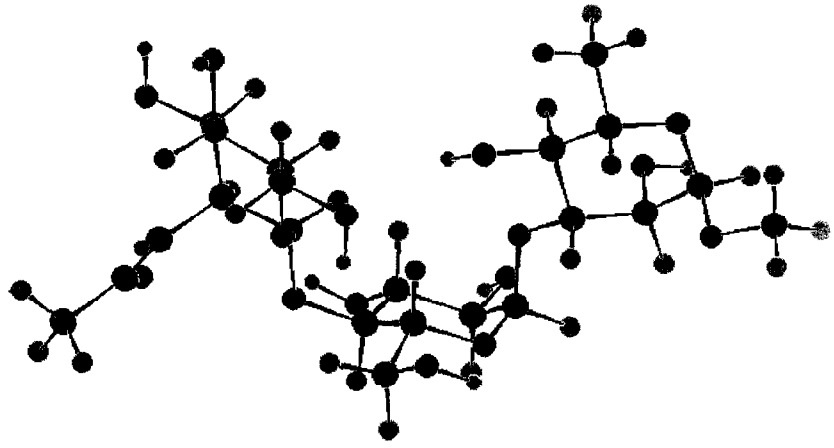

2CA

Fig. 2. (continued).

The trisaccharides **1** and **2** were synthesised as amorphous powders, according to the published procedures [2] starting from 4-(2-acetamido-6-*O*-acetyl-3,4-di-*O*-benzyl-2-deoxy-β-D-mannopyranosyl)-6-*O*-acetyl-2-*O*-benzyl-α-D-glucopyranosyl bromide [2] and benzyl 3,4-di-*O*-benzyl-α-L-rhamnopyranoside [9] or benzyl 2,4-di-*O*-benzyl-α-L-rhamnopyranoside [9].

Compound **1** had $[\alpha]_D^{20}$ +21.5° (*c* 0.8, MeOH). *Anal.* Calcd for $C_{21}H_{37}NO_{15}$: C, 46.41; H, 6.81; N, 2.58. Found: C, 46.24; H, 6.96; N, 2.40.

Compound **2**, had $[\alpha]_D^{20}$ +12.6° (*c* 0.8, MeOH). *Anal.* Found: C, 46.20; H, 6.75; N, 2.65.

Prior to the NMR analysis, each sample was freeze-dried twice from D_2O; the ^1H-NMR data are reported in Table I.

REFERENCES

1 H.J. Jennings, K.-G. Rosell, and D.J. Carlo, *Can. J. Chem.*, 58 (1980) 1069–1074; N. Ohno, T. Yadomae, and T. Miyazaki, *Carbohydr. Res.*, 80 (1980) 297–304; E. Katzenellenbogen and H.J. Jennings, *ibid.*, 124 (1983) 235–245.
2 L. Panza, F. Ronchetti, G. Russo, and L. Toma, *J. Chem. Soc., Perkin Trans. I*, (1987) 2745–2747; L. Panza, F. Ronchetti, and L. Toma, *Carbohydr. Res.*, 181 (1988) 242–245.
3 I. Tvaroška, *Pure Appl. Chem.*, 61 (1989) 1201–1216; B. Meyer, *Top. Curr. Chem.*, 154 (1990) 141–208.
4 K. Bock, *Pure Appl. Chem.*, 55 (1983) 605–622.
5 J.C. Tai and N.L. Allinger, *J. Am. Chem. Soc.*, 110 (1988) 2050–2055.
6 A. Neuman, H. Gillier-Pandraud, and F. Longchambon, *Acta Crystallogr., Sect. B*, 31 (1975) 2628–2631.
7 G.A. Jeffrey; R.K. McMullan, and S. Takagi, *Acta Crystallogr., Sect. B*, 33 (1977) 728–737.
8 S. Takagi and G.A. Jeffrey, *Acta Crystallogr., Sect. B*, 34 (1978) 2551–2555.
9 A. Lipták, P. Fügedi, and P. Nánási, *Carbohydr. Res.*, 65 (1978) 209–217.